

Species-specific densities of states of Ga and As in the chemisorption of oxygen on GaAs(110)

K. D. Childs and M. G. Lagally

Department of Metallurgical and Mineral Engineering and Materials Science Center, University of Wisconsin, Madison, Wisconsin 53706

(Received 18 October 1983; revised manuscript received 2 July 1984)

Auger line-shape measurements have been made to extract the variation in the local charge distribution around Ga and As sites for chemisorption of oxygen on cleaved and sputter-etched GaAs(110). A significant variation with changing oxygen coverage is observed in the Ga spectrum, with a much more subtle change in the As spectrum. The kinetics of oxygen chemisorption on the sputter-etched surface is much more rapid than that on the cleaved surface. The line-shape changes induced by oxygen on the two surfaces are, however, similar. Conclusions on the nature of the bonding and on the mechanism for adsorption at both low and high coverages are drawn.

I. INTRODUCTION

Because of the possible technological importance of oxides on III-V compounds, the adsorption of oxygen on GaAs surfaces has been extensively investigated. In particular, the adsorption site and the nature of the chemical interaction between O and the Ga or As atoms on GaAs(110) have generated considerable experimental and theoretical effort. The results of these studies can be summarized as follows. It is generally believed, on the basis of electron-energy-loss spectroscopy (EELS), low-energy electron diffraction (LEED), and x-ray or ultraviolet photoelectron spectroscopy (XPS or UPS), that both Ga and As atoms in GaAs(110) participate in bonding to O.¹⁻⁷ Two adsorption regimes appear to exist, with a dividing line roughly at a coverage Θ of 0.1 ML (where ML denotes monolayers).^{5,6} If a molecularly adsorbed state exists at all, it exists only below this coverage, i.e., the chemisorption of O is dissociative over most and possibly all of the coverage range.¹⁻⁹ Defects on the surface appear to be important both in providing initial adsorption sites and in the dissociation of O₂ molecules, causing the chemisorption of atomic oxygen even if care is taken to avoid atomic oxygen in the exposure.⁵⁻¹¹ Atomic or excited oxygen is adsorbed at a much faster rate than molecular oxygen.^{2,9,12} A surface with a high defect density adsorbs oxygen faster than one with a low density.^{4,5,10,13} These conclusions are, in the main, drawn on the basis of core-level chemical shifts and changes in valence-band photoemission and electron-energy-loss spectra as a function of O exposure, with some supporting evidence from LEED measurements. A number of models for the adsorption site and the resultant "surface molecule" have been proposed, including O bridge bonds between Ga and As surface atoms,³ separate Ga-O and As-O bonds,⁶ surface oxides,⁵ and more complex arrangements.¹⁴ Calculations indicate, however, that adsorption on one kind of site (e.g., As) may cause charge transfer between species.^{11,12,15-19} Thus it may not be straightforward to draw conclusions about bonding sites simply from chemical shifts or the behavior of energy-loss peaks.

In some calculations¹⁸ it is possible to project out the local density of states at each species as a function of the bonding geometry of the adsorbate, and to follow changes in it as a function of coverage. A measurement related to this density of states is possible by observing, for each species of interest, an Auger transition that involves the valence band. When compared to local-charge-distribution calculations, it may provide a verification of the local chemical changes that occur upon chemisorption. Because of the dipole-dipole nature of the Auger process, the probability of finding the "up" electron in an Auger transition a distance R from the initial core hole falls off as $1/R^6$, and the integrated Auger currents as $1/R^4$.²⁰ In particular, core-core-valence (CCV) Auger transitions are readily related to a species-specific valence-band density of states.^{21,22} The species specificity of the Auger process has been demonstrated experimentally for a number of materials,²¹⁻²³ and a comparison between experimental²² and theoretical²¹ results has been made for clean GaAs(110).²² We present measurements of core-core-valence Auger transitions of Ga and As as a function of oxygen coverage on both cleaved GaAs(110) and GaAs(110) that has been damaged by sputter etching. We extract from these measurements Auger line shapes that can be interpreted as a "fingerprint" of the changes in the species-specific density of states around the Ga and As sites with changing oxygen coverage.

II. EXPERIMENTAL DETAILS

The experiments were conducted in an ion-pumped ultrahigh-vacuum (UHV) system with a base pressure of 8×10^{-11} Torr on n -type, Te-doped GaAs crystals.²⁴ Samples were cleaved in vacuum, employing a knife-edge-and-anvil technique, yielding mirrorlike (110) surfaces with few macroscopic striations, and a step density, measured independently by LEED,²⁵ of less than one step in 60 lattice constants (the instrumental resolution) in any direction on the crystal surface. The disordered surface was prepared by sputter-etching the cleaved surface with a 3-keV Ar⁺-ion beam. No LEED pattern is observable

after this sputter etching. Derivative Auger signals were measured with a single-pass cylindrical mirror analyzer using 2 eV modulation and phase detection. The Ga and As $M_1M_{45}V$ lines were signal-averaged for periods between 5 and 18 min. These Auger transitions occur at kinetic energies close to the minimum of the electron mean free path, providing very good surface sensitivity. A backscattered-electron spectrum was taken at a primary-beam energy such that the elastically-scattered-electron peak occurs at about the same energy as the Auger line of interest. This backscattered-electron spectrum serves to represent the electron-energy-loss and instrument broadening functions.²⁶⁻²⁸ The backscattered-electron spectrum was deconvoluted from the data using the Van Cittert iterative deconvolution method.²⁹ Additionally, Lorentzian functions representative of the two core levels involved in the CCV transitions under investigation were deconvoluted from the data to eliminate core-level broadening from the Auger spectra. The widths of these Lorentzians were determined by measuring the relevant core-level widths using XPS.³⁰ The spectra were corrected finally for the changing energy resolution of the analyzer over the energy range of the Auger line. The result is the Auger-transition species-specific valence-band density of states. This procedure has been discussed in detail elsewhere.³¹

The cleaved and sputter-etched surfaces were exposed to doses from 10 to 10^{13} L of oxygen [1 langmuir (L) = 10^{-6} Torr sec]. All oxygen exposures, rather than being cumulative, were made on freshly cleaved or freshly sputter-etched surfaces. The source of oxygen for pressures up to about 10^{-4} Torr was an oxygen-permeation tube, with exposures typically being made in a continuous flow through mode. For pressures above 10^{-4} Torr, the chamber was backfilled with research-purity oxygen from either a 1-l atm bulb or a pressurized cylinder. Before any Auger data were taken, the chamber was pumped at least into the 10^{-9} -Torr range.

It is well known that the presence of hot filaments affects the rate of adsorption of oxygen.^{2,9,12} Exposures were made both with and without hot filaments present. The lowest exposures were predominantly made with a filament on, which in these cases was an ion gauge some distance from, and not in direct line of sight of, the sample surface. For exposures in which no hot filaments were present ($p > 10^{-4}$ Torr), the pressure was measured either with an ion gauge before the sample was cleaved, or with a thermocouple gauge, or calculated volumetrically. To obtain the coverage as a function of exposure, concentrations of O, Ga, and As were measured using the O KVV peak height and the Ga and As LMM peak heights at 512, ~ 1070 , and ~ 1230 eV, respectively, with the appropriate sensitivity factors.³² Oxygen concentrations were calculated for a model of O sitting on top of GaAs(110), assuming no rearrangement of O, Ga, or As perpendicular to the surface, and using appropriate escape depths³³ and the bulk interplanar distance of 2 Å. One monolayer corresponds to one oxygen atom for each surface Ga and As. Measured concentrations for various oxygen exposures were then compared to these calculations to estimate the resulting oxygen coverages. Figure 1(a) shows the varia-

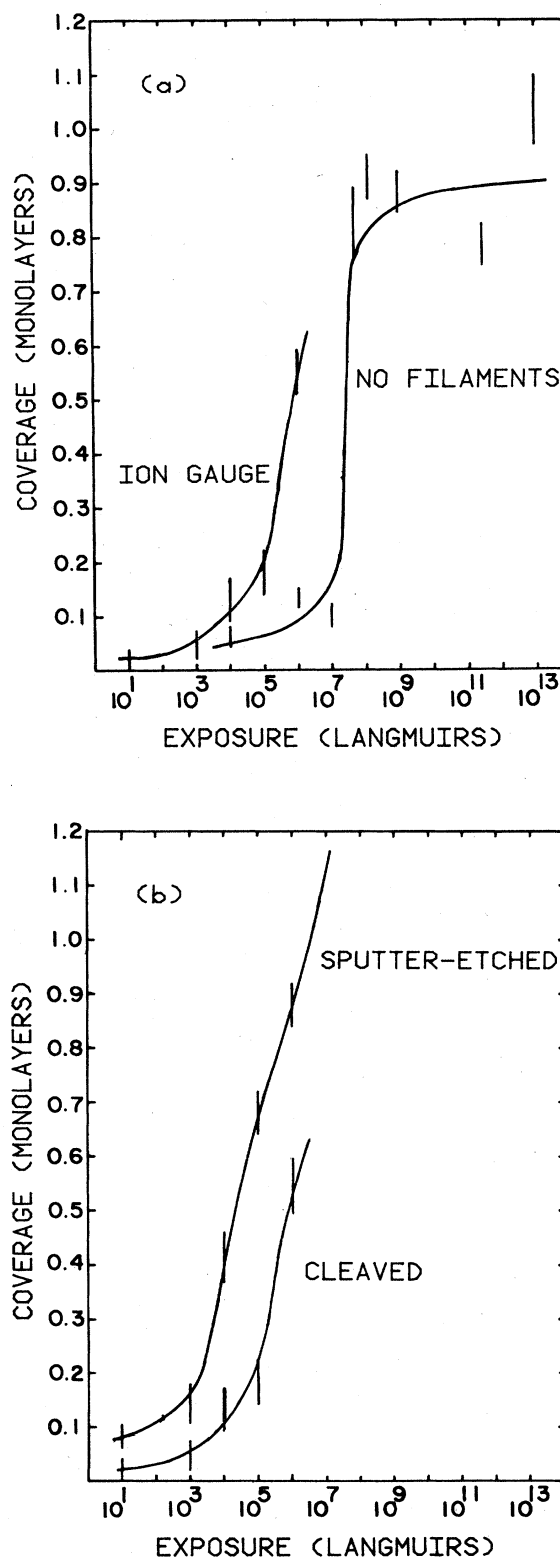


FIG. 1. Dependence of coverage on exposures for oxygen chemisorption on GaAs(110) under several circumstances. (a) Coverage on cleaved GaAs(110) with an ion gauge on and without any hot filaments on. (b) Coverage on cleaved and sputter-etched GaAs(110) for exposures made with an ion gauge on.

tion of coverage on the cleaved surface resulting from exposures with and without an ion gauge present, as previously described. Figure 1(b) is a comparison of the variation of coverage on the cleaved and sputter-etched surfaces resulting from exposures under identical conditions. The error bars in Fig. 1 are a composite of an estimate of the uncertainty in Auger peak heights due to instrumental factors and the observed variation of Auger signal in different areas on a given surface. The accuracy of the absolute coverages depends additionally, of course, on the accuracy of the electron escape depths and the relative Auger sensitivity factors in the model calculations. A $\pm 50\%$ change in the oxygen sensitivity factor results in coverages of 0.7 and 1.9 ML, respectively, at the exposure calculated above to correspond to $\Theta = 1$ ML, and a $\pm 20\%$ change in the average mean-free-path results in coverages of 0.8 and 1.3 ML, respectively. These uncertainties are not included in the error bars.

Special attention was paid to the influence of H_2O on the adsorption. H_2O adsorbs more rapidly than oxygen,³⁴ and thus it is important to know the fraction of H_2O in the ambient gas. With the use of a LN_2 cold finger, the H_2O partial pressure $p_{\text{H}_2\text{O}}$ was always 3 or 4 orders of magnitude smaller than p_{O_2} , for $p_{\text{O}_2} < 10^{-6}$ Torr. At higher p_{O_2} , the fraction of H_2O was even smaller. At these partial pressures, the influence of H_2O on the observed adsorption kinetics of O_2 is negligible.³⁴ CO adsorbs considerably more slowly and does not affect the O-coverage results, whether molecular or excited.³⁵ No C or other contamination is found, even after the largest O_2 exposures.

Electron-beam effects were carefully monitored by making Auger measurements at a variety of electron dosages, oxygen coverages, and oxygen background pressures. It was found that the surface oxygen concentration typically increased slightly in the presence of an electron beam, in the vicinity in which the electron beam impinged. A correlation was observed with the ambient pressure in the system when the Auger measurements were made: The higher this pressure, the more the surface O concentration increased for a given electron dose. (We have observed the same phenomenon for CO adsorption.) This result leads us to the conclusion that we are observing electron-stimulated adsorption of oxygen, probably through the dissociation of H_2O , and possibly also of remaining O_2 , by the beam, creating more easily adsorbable oxygen. The effect is similar to having a hot filament present, and is electron-dose dependent. If one assumes that all "activated" O created by the beam is adsorbed, one can estimate a lower limit to the sticking coefficient for this O. At 10^{-9} Torr and 1000 sec, ~ 0.2 ML is adsorbed. If the sticking coefficient s is equal to 1, the exposure to form a monolayer is 10^{-6} Torr sec. Hence, s for this activated O is at least of the order of 0.2.

For high exposures, the system was generally pumped only into the 10^{-9} -Torr range before measurements were made, while for low exposures it was possible to pump the system fairly quickly into the 10^{-10} -Torr range. Thus the change in surface concentration during exposure to the electron beam is much less at low coverages. For the

cleaved surface, the change in oxygen coverage that is observed over the time it takes to accumulate the data for one set of Auger line shapes averages $\Delta\Theta \approx 0.06$ ML, and ranges from near zero to $\Delta\Theta \leq 0.2$ ML in the worst case. The spectra shown represent an average of the line shapes over a coverage range $\Theta_{\text{initial}} + \Delta\Theta/2$. In the figures showing line shapes, the referenced coverages are always the average values.

In addition to the *LMM* lines, the Ga and As $M_3M_{45}M_{45}$ Auger peak heights, at ~ 50 and ~ 30 eV, respectively, were monitored for coverage determinations. The *MMM* lines should be more surface sensitive than the *LMM* lines; however, they vary considerably in intensity and thus are not reliable. Within the error, both sets of lines indicate that, for the cleaved surface, the $[\text{Ga}]/[\text{As}]$ ratio remains 1:1 for all oxygen exposures.³⁶ For the clean, sputtered-etched surface the nominal $[\text{Ga}]/[\text{As}]$ ratio is approximately 3:2 and remains 3:2 for all oxygen coverages $\Theta \leq 1$ ML. There is a definite decrease in the As signal from the sputter-etched surface for exposures resulting in $\Theta > 1$ ML. For exposures of 10^{11} L there is little As left in the sample volume contributing to the Auger signal.

Comparison of the oxygen-coverage-versus-exposure curves in Fig. 1(a) shows that the presence of filaments increases the adsorption rate^{2,9,12} and also changes the shape of the curve. Additionally, Fig. 1(b) shows that the kinetics are more rapid on the sputter-etched surface than on the cleaved surface, supporting earlier suggestions about the influence of defects.^{4,5,10,13} For the highest exposures (10^{11} and 10^{13} L, no filaments on), the coverage on the cleaved surface shows a tendency toward saturation at about 1 ML, while the sputter-etched surface shows no such tendency, but results in the formation of a region depleted of As, but rich in Ga and O.

III. CHEMISORPTION OF OXYGEN ON CLEAVED GaAs(110)

Auger line-shape measurements for Ga and As atoms in the cleaved surface have previously been made²² and compared to calculations.²¹ Figure 2 shows the species-specific transition-valence-band densities of states for Ga and As derived from the $M_1M_{45}V$ transitions.³⁷ The Ga and As $M_1M_{45}V$ lines occur, respectively, between 115 and 135 eV and between 135 and 160 eV. Spectra 1 and 2 are the line shapes resulting from the use of two extreme conditions in the deconvolution routine on one set of data. Spectra 2–6 are results for four cleaves and for two locations on one cleavage face. Spectrum 7 shows data taken with 1 eV modulation. A comparison of all of these spectra demonstrates that the data are reproducible from one sample to the next, and that variation of parameters in the data-reduction procedure over physically reasonable limits does not affect the final line shapes significantly. In addition to the kinetic-energy scale, an energy scale referenced to the valence-band edge is shown in Fig. 2. This scale was determined by rigidly aligning the experimental profiles with the theoretical curves.²¹ The resulting peak energies agree very well with those determined by XPS,²² although, as has been observed for all other Auger line

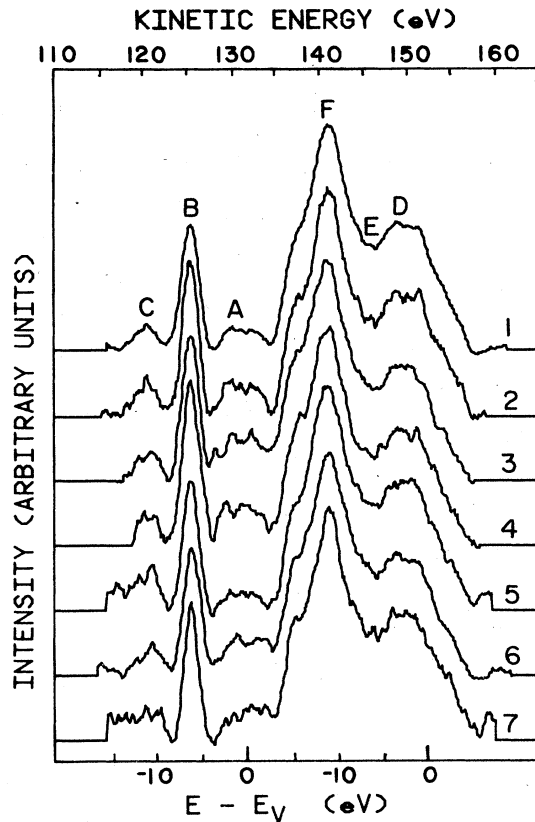


FIG. 2. $M_1M_{45}V$ Auger line shapes for Ga and As in clean, cleaved GaAs(110). Ga lies between 115 and 135 eV and As between 135 and 160 eV. The bottom scale is referenced to the valence-band edge for each line. It is obtained by rigidly aligning this spectrum with the corresponding calculation (Ref. 21). The spectra were obtained from four separate cleaves and two locations on one cleavage face. Spectra 1 and 2 are the results for two extreme conditions in the data-reduction procedure on one data set; spectra 2 and 3 are for different locations on one surface, and spectra 3–6 are for different cleaves. Spectrum 7 was obtained using 1 eV modulation; all others were taken with 2 eV modulation. A–F label spectral regions that are discussed in the text.

shapes,^{22,23,31} a broadening of the line occurs. The Ga-specific density of states consists of three peaks. Peak A at the top of the spectrum is *p*-like, B at –6 eV is *s*-like, and C at –11 eV is of mixed character.²¹ The As-specific density of states also has three features: peak D at the top of the As valence band is *p*-like, peak F at –11 eV is *s*-like, and the region E between D and F is *p*-like.²¹ Matrix-element considerations cause the *s*-like states to dominate the valence-band spectra determined from $M_1M_{45}V$ transitions in these elements.²¹

Figures 3(a) and 3(b) show the $M_1M_{45}V$ -derived Ga- and As-specific densities of states for different oxygen coverages on the cleaved surface resulting from exposures made with no filaments on. Figures 4(a) and 4(b) are equivalent results for exposures made with the ion gauge on. The Ga and As spectra are separately normalized to their clean-surface values so that the area under each line remains constant at different coverages. The Ga-specific

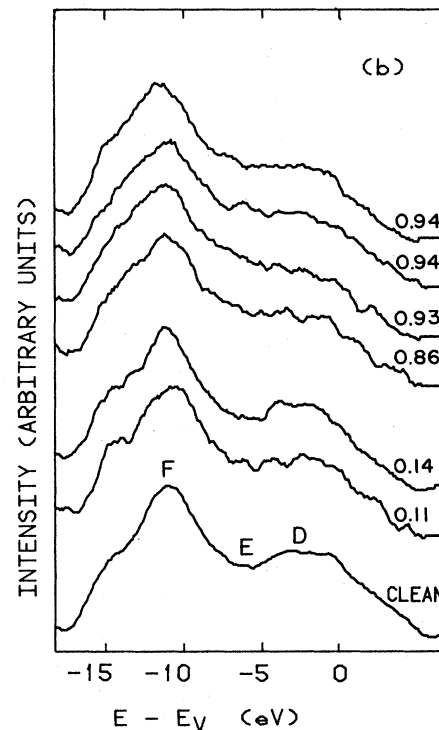
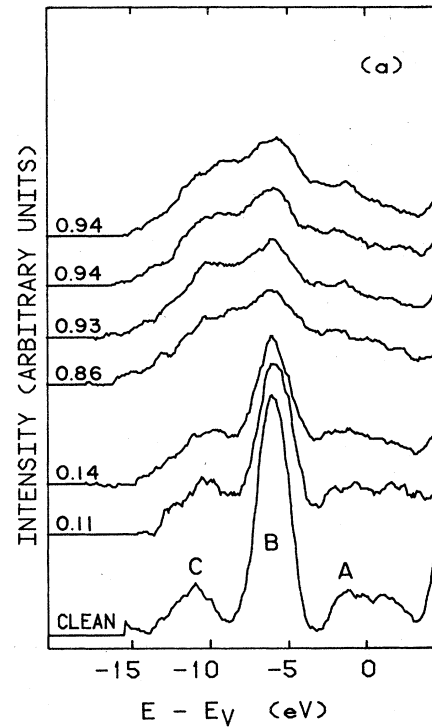


FIG. 3. Variation in the Ga- and As-specific densities of states as a function of oxygen coverage on cleaved GaAs(110); (a) Ga and (b) As. Exposures were made with no filaments on. The integrated intensities in the Ga and As spectra are separately normalized to those of the clean surface. The oxygen coverages are listed in fractions of a monolayer. Because of the rapid change in coverage with exposure, Fig. 1, it was not possible to obtain spectra in the region of $\Theta \sim 0.5$ ML.

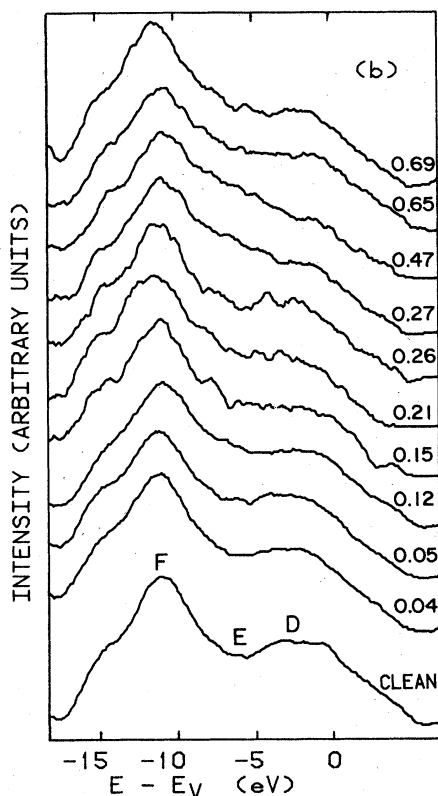
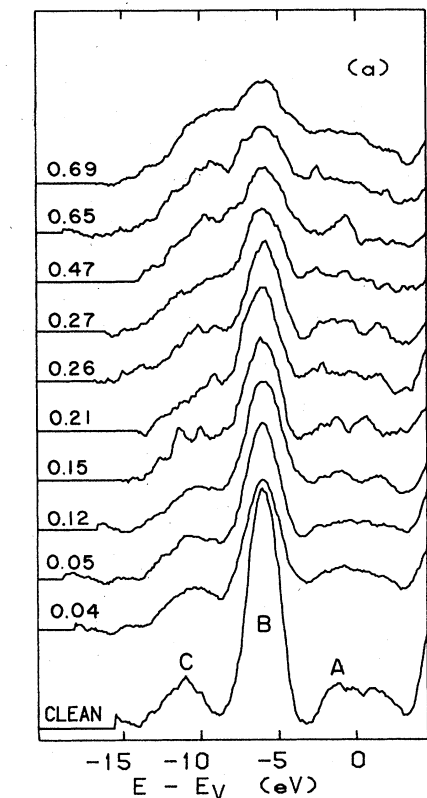


FIG. 4. Ga- and As-specific densities of states as in Fig. 3, except that exposures were made with an ion gauge on.

density of states undergoes dramatic changes with increasing coverage. In Fig. 3(a), at $\Theta \sim 0.1$ ML, changes in the Ga shape relative to the clean surface are evident: peak *B* markedly decreases in intensity relative to peaks *A* and *C*, and broadens. At $\Theta \sim 0.14$ ML, the intensity at the top and bottom of the Ga spectrum has increased slightly relative to a further-broadened peak *B*. At $\Theta \sim 0.86$ ML, the intensity between peaks *B* and *C* has substantially increased relative to peak *B*. The Ga spectrum then changes very little for coverages between $\Theta \sim 0.86$ and 0.94 ML. The Ga spectra for exposures with no filaments on [Fig. 3(a)] are essentially the same at similar coverages as those taken with a filament on [Fig. 4(a)]. For example, the spectra for $\Theta = 0.11$ and 0.14 ML are comparable in the two figures. The relative intensity of the feature at -9.5 eV for $\Theta \sim 0.86$ ML in Fig. 3(a) is somewhat greater than that for $\Theta \sim 0.65$ ML in Fig. 4(a), as might be expected from the larger oxygen coverage. We conclude that, although the adsorption kinetics are affected, the local bonding and absorption sites must be similar for both situations. The changes in the As-specific density of states [Figs. 3(b) and 4(b)] with changing O coverage are small compared to those for Ga. The intensity of peak *D* decreases, with a concomitant increase at *E* in the middle of the spectrum. These changes appear to be continuous from the lowest coverage on, unlike the changes in the Ga line. Again, the spectra for exposures with and without filaments on are similar at similar coverages.

IV. CHEMISORPTION OF OXYGEN ON SPUTTER-ETCHED GaAs(110)

Chemisorption experiments were also performed on sputter-etched surfaces. Sputter-etching introduces an extreme degree of structural disorder in the surface region. The LEED pattern of such a surface is obliterated, indicating that ordered-domain sizes are less than three atoms in diameter.²⁵ There is thus at best only very-short-range order in the sputter-etched surface. The composition of the sputter-etched GaAs "surface" is (58 ± 2) at. % Ga and (42 ± 2) at. % As, measured using the Ga and As *LMM* and *MMM* Auger peak heights, as already mentioned, and the same sensitivity factors as for the clean, cleaved surface. Because GaAs can exist as a single phase over only a very narrow composition range, 49.935–50.015 at. % Ga,³⁸ any Ga in excess of this range will form a second phase. This second phase appears as Ga "beads" that are of the order of $1 \mu\text{m}$ in diameter or smaller, covering about 20% of the sputter-etched surface.³⁹ Up to a monolayer of excess Ga uniformly covering the surface cannot be excluded on the basis of the bulk phase diagram,³⁸ but appears to be inconsistent with the composition measurements, given the areal density of Ga "beads."

To illustrate the effect of sputter etching on the local electronic properties, Fig. 5 shows a comparison of the $M_1M_{45}V$ -derived Ga- and As-specific densities of states from clean cleaved and sputter-etched GaAs(110), along with the $M_1M_{45}V$ -derived density of states from sputter-etched elemental Ga. The major influence of sputter etching on the Ga-specific density of states in GaAs(110) is an increase in intensity at the top of the valence band, and an

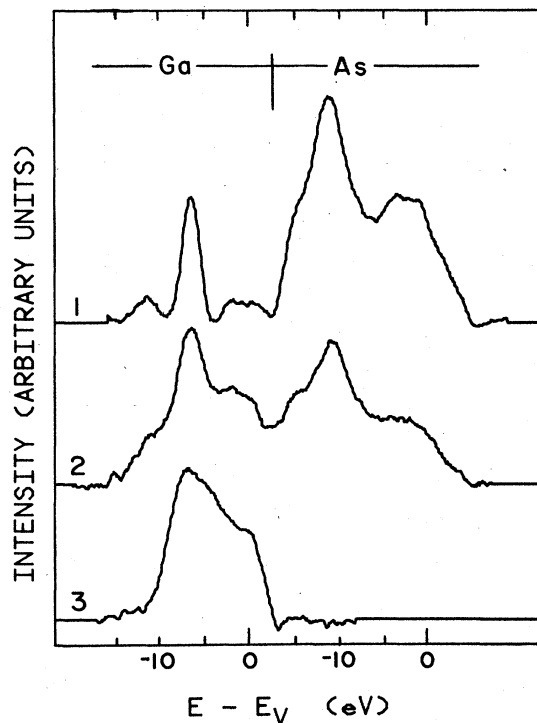


FIG. 5. Illustration of elemental Ga component in the Ga spectrum from sputter-etched GaAs(110). 1, cleaved GaAs(110); 2, sputter-etched GaAs(110); 3, sputter-etched elemental Ga. Spectra 1 and 2 are normalized to the same total area; spectrum 3 is normalized to half of that value.

overall broadening of the line shape due to the disorder introduced in the GaAs phase.³⁹ Figure 5 shows that the Ga line in sputter-etched GaAs(110) can be considered to be the superposition of lines for pure Ga and for Ga in stoichiometric GaAs(110). The As-specific density of states shows an overall broadening. The integrated intensity in the As line shape is reduced relative to that of Ga because of the loss of As from the surface layers upon sputter etching.

The $M_1M_{45}V$ -derived Ga- and As-specific densities of states for different oxygen coverages on the sputter-etched surface are shown in Figs. 6(a) and 6(b). The Ga and As spectra are again separately normalized to their clean-surface values to maintain constant area under each curve for different coverages. The curves are thus directly comparable to those of Figs. 3 and 4. There are no detectable changes in the Ga-specific density of states relative to the clean surface for coverages up to $\Theta \sim 0.15$ ML, in contrast to the results on the cleaved surface. On the other hand, the features that develop in the Ga spectrum for the cleaved surface at low O coverages are already present to some degree on the clean, sputter-etched surface. At higher O coverages, the behavior is similar to that of the cleaved surface. In particular, the peak that grows with increasing oxygen coverage between peaks B and C in the spectrum from the cleaved surface does so for the sputter-etched surface as well. The influence of increasing O coverage on the As spectrum for the sputter-etched surface is similar to that on the cleaved surface, i.e., a de-

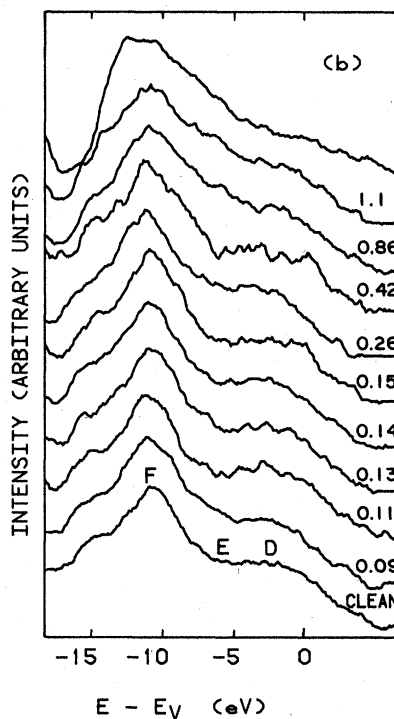
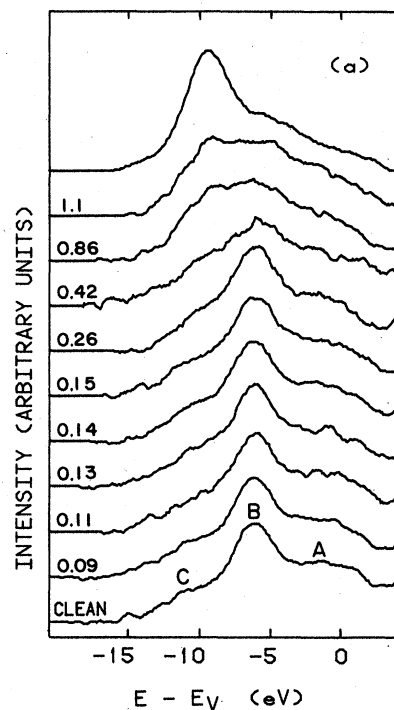


FIG. 6. Variation of the Ga- and As-specific densities of states as a function of oxygen coverage on sputter-etched GaAs(110); (a) Ga and (b) As. The integrated intensities in the Ga and As spectra are separately normalized to those of the clean surface. The oxygen coverage is listed in fractions of a monolayer. The top spectra are for an exposure of 10^{11} L, which results in a surface layer rich in Ga and O and depleted of As.

crease in intensity at D and an increase at E . No change is observed below $\Theta \sim 0.15$ ML. For exposures of 10^{11} L or more, the total intensity in the As $M_1M_{45}V$ line is greatly reduced as the surface becomes depleted of As, and the peak at -9.5 eV dominates the Ga spectrum.

V. DISCUSSION

In this section we summarize and compare the results of the preceding two sections and discuss the implications of these results.

Oxygen adsorption on the cleaved surface causes significant changes in the Ga-specific density of states already at the lowest measurable coverages. The line shape [Figs. 3(a) and 4(a)] changes rapidly with coverage initially, then more slowly as the coverage increases to nearly a monolayer, suggesting the existence of two regimes in the chemisorption of oxygen, in agreement with earlier work.^{5,6} The As-specific density of states [Figs. 3(b) and 4(b)] changes much more subtly and continuously from $\Theta=0$ to $\Theta \sim 1$ ML. The kinetics of adsorption resulting from exposures to molecular oxygen (no filaments on) slow dramatically for exposures above $\sim 10^7$ L ($\Theta \geq 0.8$ ML), with a slow increase in O coverage for exposures beyond that. It appears that both Ga-O and As-O bonds form, because both lines show changes. The trend in the Ga line shape with increasing coverage can be interpreted in terms of an increasing contribution from the spectrum of Ga in Ga_2O_3 . This is illustrated in Figs. 7 and 8. Figure 7 shows a comparison of Ga spectra taken for elemental Ga and for GaAs(110). Spectra 1 and 6 are, respectively, clean elemental Ga and clean, cleaved GaAs(110). Spectrum 2 is representative of oxide on Ga; from thermodynamic considerations, this oxide is expected to be Ga_2O_3 .⁴⁰ The most notable feature in spectrum 2 is a peak at -9.5 eV: this peak is also the one that grows upon O chemisorption on GaAs(110), a conclusion that can be confirmed from spectra 3–5, as well as from Figs. 3(a), 4(a), and 6(a). We do not believe that this feature is due to the density of states on the oxygen atom. Auger-electron spectroscopy (AES) is a local probe, but one could imagine the O atom sitting close enough to the Ga atoms for O wave-function overlap to occur onto the Ga core. However, if the O feature were observed in the Ga spectrum, it should, in all likelihood, also be observed in the As spectrum, unless the O atoms were significantly closer to the Ga atoms. Figure 8(a) shows that Ga spectra measured at different O coverages can be approximated with a superposition of Ga lines from Ga_2O_3 and clean, cleaved GaAs(110). The trends in the line shapes are reproduced, demonstrating that the change in the Ga spectrum with increasing O coverage can be attributed to an increasing Ga_2O_3 component. The fit can be made much better if the Ga line shape for $\Theta \sim 0.04$ ML rather than for the clean, cleaved surface is used, as shown in Fig. 8(b). This also supports the notion that there are two regimes of adsorption, with a division at $\Theta \leq 0.05$ ML. One can conclude that the electronic charge distribution around those Ga sites in cleaved GaAs(110) at which O is chemisorbed is similar to that around Ga in bulk Ga_2O_3 . The determination of similarity to Ga_2O_3 is not unique, because we have not looked at a large variety of Ga oxides

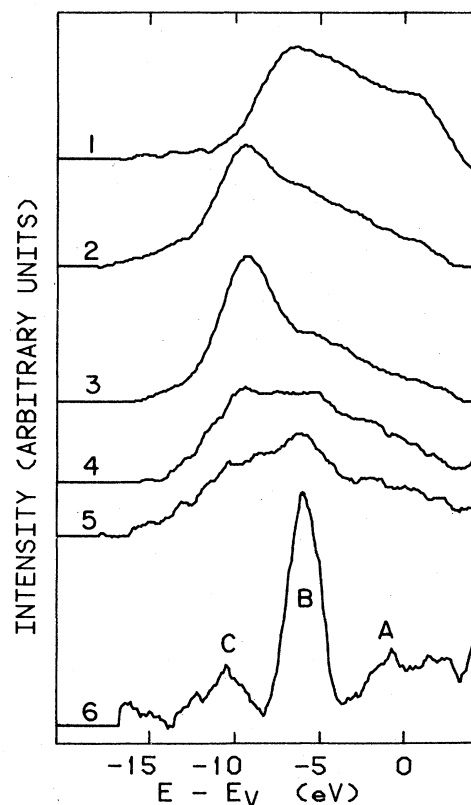


FIG. 7. Comparison of several Ga spectra to illustrate the contribution of oxide to the line shape: 1, clean elemental Ga; 2, Ga oxide, expected to be Ga_2O_3 ; 3, oxide layer on sputter-etched GaAs(110) from top curve, Fig. 6(a); 4, $\Theta \sim 1.1$ ML on sputter-etched GaAs from Fig. 6(a); 5, $\Theta \sim 0.93$ ML on cleaved GaAs from Fig. 3(a); and 6, clean, cleaved GaAs(110).

to see if they produce different Ga Auger lines.

From Fig. 8 one can also conclude that the mechanism for oxygen bonding does not change over the coverage range studied. The area under the "oxide" contribution to the spectrum can be considered as the oxygen "coverage" on the Ga sites. If the change in this area is compared to the total O coverage, it is found that the two scale. Hence there can be no change in the bonding geometry that would produce a significant difference in charge distribution. It is not, for example, possible for bonding to occur initially on Ga sites and later on As sites.

The model of Ludeke³ for the equilibrium positions of O atoms adsorbed on the GaAs(110) surface, consisting of oxygen bridge bonds to surface Ga and As atoms, most closely matches the constraints imposed by our data,⁴¹ with the implicit assumption of negligible charge transfer between Ga and As that has been frequently made.^{2,4-6} Simpler models do not appear to be satisfactory. We have made attempts to match our spectra with layer-averaged charge densities produced in calculations for simple models,¹⁸ but have not found it possible to draw a correspondence in the trends of the experimental and theoretical spectra.

Oxygen adsorption on a sputter-etched surface causes observable changes in the line shapes, Figs. 6(a) and 6(b),

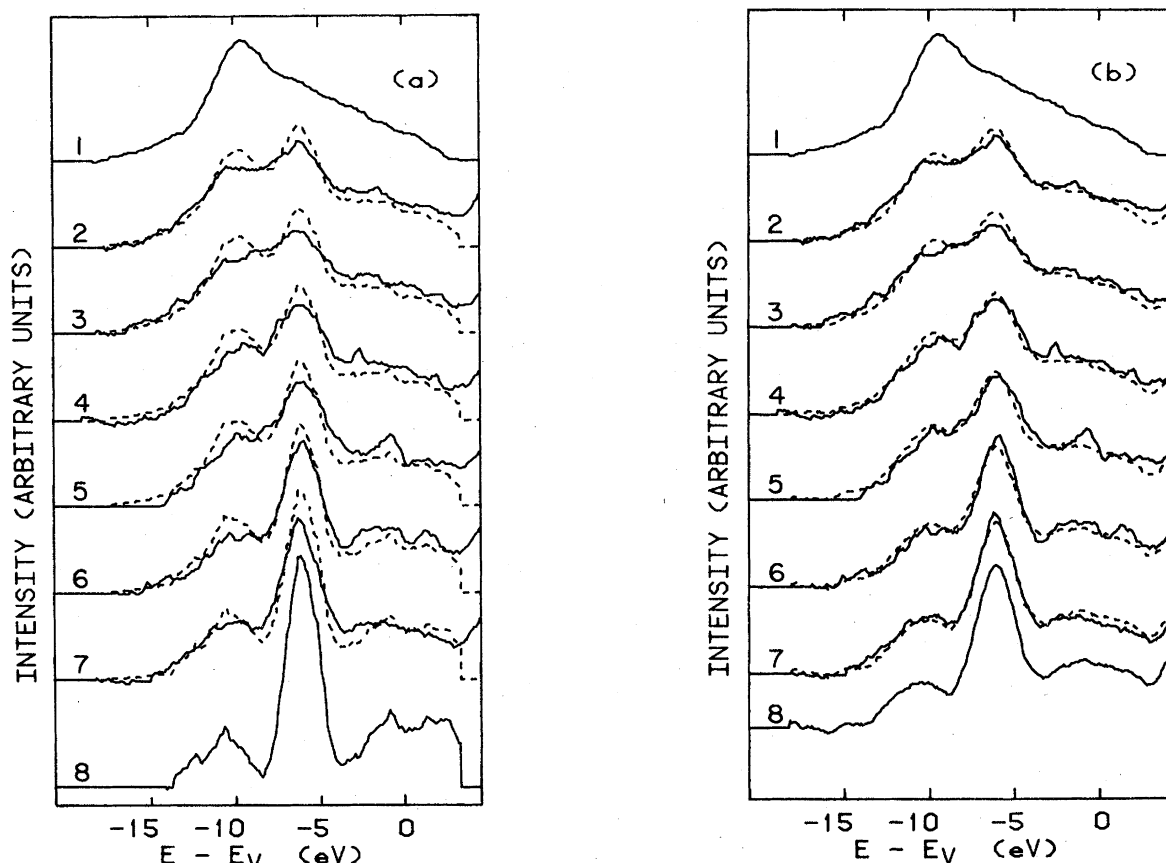


FIG. 8. Fits of the spectra at different oxygen coverages (in ML) on cleaved GaAs(110) with a model to account for the oxide contribution. Solid curves, measurement: 1, Ga oxide; 2, 0.93; 3, 0.86; 4, 0.65; 5, 0.47; 6, 0.26; 7, 0.14. These spectra are the same in both panels. Dashed curves, model calculations of oxide contribution. (a) Fits are made by summing spectrum 1 and spectrum 8, for clean, cleaved GaAs(110), in amounts proportional to the O coverage. (b) Fits are made by summing spectrum 1 and spectrum 8, for $\Theta=0.4$ ML, in amounts proportional to the O coverage.

only for $\Theta > \sim 0.15$ ML. The changes in the spectra beyond this coverage are similar to those occurring on the cleaved surface. This implies that the local surface chemical arrangement becomes similar in both surfaces above this coverage. This can be understood in the following way. The sputter-etched surface is depleted of As over the entire coverage range. It is therefore reasonable that at a given oxygen coverage, there will be more Ga—O bonds on the sputter-etched surface than on the cleaved surface. On the sputter-etched surface two chemisorption processes initially compete: adsorption onto the Ga “beads” and attack of Ga and As bonds in the disordered GaAs. It is presumably easier to chemisorb O on the Ga “beads,” forming Ga_2O_3 , and thus this process occurs preferentially. As this reaction saturates, the chemical environment in the initially ordered and initially disordered GaAs surfaces must become the same. Spectra 4 and 5 in Fig. 7 show the Ga spectra for $\Theta \sim 1.1$ ML on the sputter-etched surface and for $\Theta \sim 0.93$ ML on the cleaved surface. The types of bonds that are formed on Ga and on GaAs (both cleaved and sputter-etched) must be very similar, i.e., the Ga atoms must be strongly involved and the “surface compound” that is formed must look, to Ga, like a Ga oxide. If this were not the case, i.e., if the bonding of O on Ga were different from that on GaAs, the differences that exist in the clean-surface spec-

tra would continue to manifest themselves for all coverages.

In Figs. 3, 4, and 6 the spectra were separately normalized to their zero-coverage value. This allows only an observation of the redistribution of charge density at each site, and not of the change in the charge density with coverage. The data are plotted to permit the latter view in Figs. 9 and 10 for the cleaved and sputter-etched surfaces, respectively. Here the spectra are normalized so that the sum of intensities under the Ga and As lines remains constant with changing coverage. Although Auger spectra do not give a species-specific density of states directly, but rather a transition density of states that depends on matrix elements and the fact that the final state is an ion, these factors should not depend on coverage. We therefore believe that the changes in the spectra shown in Figs. 9 and 10 can be interpreted in terms of a changing relative local charge density. The total charge around each species can be taken to be proportional to the integral under the line, as long as the stoichiometry does not change. (It should be recalled that it does not change below $\Theta=0.8$ ML.) It is evident from Figs. 9 and 10 that there is an increase in electron density around Ga sites relative to As sites with increasing O coverage.

There may be two causes for a change in the local charge density around each species with increasing oxygen

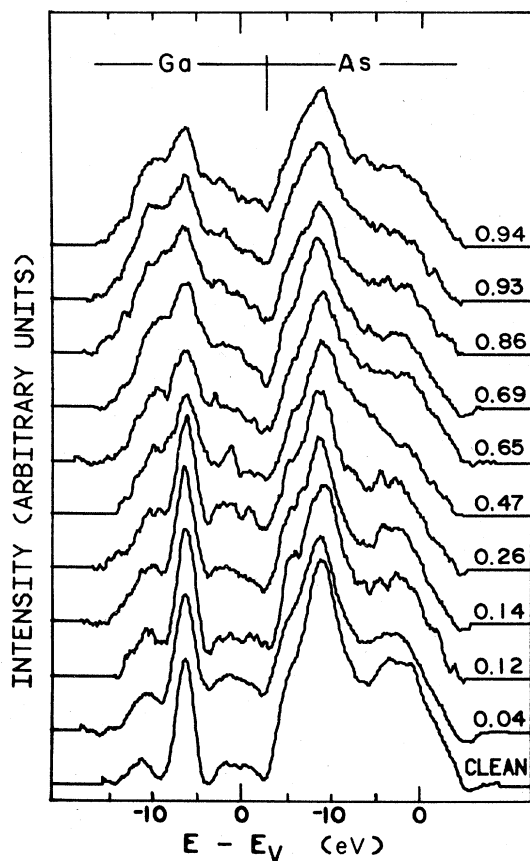


FIG. 9. Variation of the Ga- and As-specific densities of states as a function of oxygen coverage on cleaved GaAs(110). The area under each curve (Ga and As combined) is normalized to that of the clean surface to illustrate the change in the relative charge density at each species. The oxygen coverages are listed in fractions of a monolayer.

coverage. The chemical bond with oxygen in all likelihood is itself preferential in the sense that O contributes charge differently to Ga and As. Additionally, charge may flow between the Ga and As species when O bonds to one or the other. It is not possible in our data to separate these two effects, and it may not even be meaningful to attempt to do so in general. If charge transfer plays the major role in determining changes in the species-specific charge density, it becomes impossible to predict, on the basis of Auger line-shape changes, which species the O atom bonds to, and thus also impossible to determine the bonding site. This is also true for core-level chemical-shift and EELS measurements, although this fact is seldom explicitly acknowledged. Calculations¹⁸ that include this charge transfer for the surface layer of GaAs with O adsorbed on either the Ga or As atoms show a large increase in the density of states at the bottom of the valence band of GaAs if O adsorbs on As, but a much smaller change if O adsorbs on Ga. We do observe a change at the bottom of the valence band, but only for the Ga-specific density of states. At first glance one would draw the conclusion that O bonds to As and that charge is transferred back to Ga. This may be the case, but the

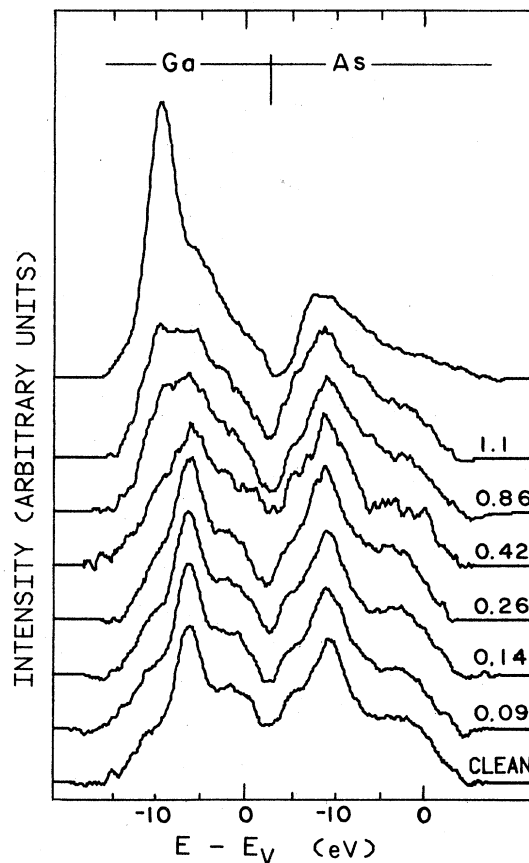


FIG. 10. Variation of Ga- and As-specific densities of states as in Fig. 9, except that the spectra are for sputter-etched GaAs(110).

conclusion cannot be drawn unequivocally without a projection of the densities of states in the calculations onto the Ga and As atoms separately, because both Ga and As have states at the bottom of the valence band.²¹ Furthermore, calculations are required for a variety of oxygen-atom positions to affirm this conclusion. These calculations would need to demonstrate a large change in the Ga density of states and a very much more subtle change in the As density of states.

In any case, it is not possible at this stage to say unequivocally that O adsorbs on one or the other or on both Ga and As sites. However, Fig. 8 shows that the Ga density of states has a component that resembles Ga_2O_3 , which increases with oxygen coverage. In pure Ga_2O_3 there obviously is no As from which charge can transfer. Thus, at least in this case, the changes that are observed can be produced purely by the presence of O at the Ga site, and there is no need to invoke charge transfer. The calculations proposed above should also be able to demonstrate this fact. An interesting observation from Figs. 3, 4, and 6 is that the changes in the local charge distributions are similar (at least above $\Theta=0.15$ ML, as discussed earlier) on the cleaved and sputter-etched surfaces, even though the adsorption kinetics are quite different. This implies that the bonding on these two surfaces is similar, irrespective of questions of charge transfer. A model con-

sistent with this fact is that oxygen chemisorption is essentially a defect-related mechanism^{4,5,7,9,10} at all coverages, i.e., that the formation of O bonds creates a disordered surface. The mechanism of chemisorption may be pictured in the following manner. Chemisorption is initiated at already existing surface defects, with the chemisorption rate determined by the concentration of such defects. On the cleaved surface, the concentration of initial defects may be quite low, depending on the quality of cleave. The chemisorption process causes further disorder, presumably through the insertion of oxygen atoms into Ga and As back bonds. Subsequent chemisorption takes place at the edge of these disordered regions, which can be thought of as nucleating on initial structural defects and growing outward from them. At an intermediate stage of chemisorption, the surface can be thought of as resembling "swiss cheese," with islands of surface disorder surrounded by structurally perfect GaAs surface. This model of the surface structure can, in principle, be checked by LEED angular profile analysis.⁴² The regions of disorder will produce only diffuse intensity, but, if they are arranged in patches, they will remove intensity from the diffracted beams in a characteristic way that depends on the size distribution and arrangement of those patches. The resulting diffracted-beam line shape then directly reflects this distribution.⁴³ Although visual observations of LEED beams have been made,⁹ we are not aware of any attempts to measure actual diffracted-beam line shapes for this system. The adsorption kinetics should also reflect this mechanism. If all initial defect sites are occupied and islands of disorder subsequently grow from them, the kinetics should be different from those resulting if O can randomly chemisorb anywhere on the surface. In the former case, the O coverage should be time dependent (and proportional to the boundary length of disordered regions), while in the latter case it should be independent of time and dependent only on the pressure-time product. The shape of the coverage-versus-exposure curve for adsorption on the cleaved surface [Fig. 1(a)], although not sufficiently detailed to distinguish different models for the adsorption kinetics, is at least not inconsistent with a model of adsorption kinetics that are obtained with the nucleating and growth of islands.⁴⁴

The sputter-etched surface is partially covered with Ga "beads" on which chemisorption probably occurs preferentially, but the defect density over the remainder of the surface is also higher than on the cleaved surface. Therefore the rate of chemisorption should be much greater on the sputter-etched surface both initially and over the entire coverage range, as is observed. If the defect density is sufficiently high, the kinetics should be dependent only on the exposure and not dependent on the time or pressure separately.

The increase in oxygen concentration above 1 ML with increasing exposure on the sputter-etched surface can also be explained on the basis of defects. The sputter-etched surface has such a high degree of disorder, and a resulting high density of broken bonds, that oxygen can probably attack to a depth of many average layer distances, allowing "bulk" oxidation to take place readily without a significant "structural" activation barrier. This "bulk" ox-

idation is evidenced by the shape of the Ga spectrum for high O exposures and the depletion of As in the surface region, as was shown in Figs. 6, 7, and 10. It is apparent that a Ga oxide has formed.

The behavior of the line shapes at very low coverages may reflect mechanisms related to Fermi-level pinning. At coverages of $\Theta \sim 0.05$ ML there is no measurable influence of oxygen adsorption on Ga or As core levels,¹⁻⁵ although there is a clear influence on the Ga Auger line shape. In this coverage region, Fermi-level pinning is observed due to the adsorption of oxygen (as well as many other species).^{1,2,4} Our results give evidence that Fermi-level pinning is in some manner associated with changes in the charge density around Ga. Fermi-level pinning has also been reported to occur for poorly cleaved surfaces or sputter-etched surfaces that have not been fully annealed.^{2,4} We observe a Ga line shape for either GaAs that has been poorly cleaved or for sputter-etched and annealed GaAs(110) that is similar to the Ga line shape for a low oxygen coverage on well-cleaved surfaces, giving additional support for the conclusion that Ga atoms are preferentially involved in Fermi-level pinning.

V. CONCLUSIONS

We have reported measurements of changes in the species-specific densities of filled states in the chemisorption of oxygen on GaAs(110) by using Auger line shapes of transitions that involve the valence band. We have demonstrated that a "fingerprint" of the charge density around individual species in a multicomponent system can be obtained as a function of coverage by measuring these line shapes. There are, of course, difficulties with an absolute interpretation of such a line shape, as there is with all electron spectroscopic measurements. First, the matrix elements for the transitions are, in general, not accurately known. Second, the final state in the Auger process is an ion, and thus the measurement does not represent the ground-state charge density. Third, relaxation effects may be important. They should be much less of a problem in GaAs than for materials with sharply peaked densities of states, such as *d*-band metals. None of these factors should significantly affect the changes in the spectra with coverage, and hence we believe that these changes can be directly interpreted as changes in the local charge configuration. The Auger line, of course, gives an average over several layers. At the energies of these lines, the mean free path is such (7 Å) that the surface layer contributes only about one-fourth of the intensity. If one assumes that the charge distribution changes only in the outer layer, these changes must be much larger than indicated in the spectra presented here.

We have demonstrated that the Ga line can be considered to be a superposition of Ga in Ga₂O₃ and Ga in GaAs. If no charge transfer between Ga and As is assumed, the model of Ludeke³ for the equilibrium position of O atoms is consistent with the constraints imposed by our results. Charge transfer may, however, be important. We hope that our measurements will stimulate further theoretical work on the subject. We conclude that oxygen chemisorption is essentially a defect-related mechanism at

all coverages, and that a correlation of structural defects with measurements of localized electronic properties such as those reported here will provide information on Fermi-level pinning. Analysis of surface structural defects, even at quite low concentrations, is possible using LEED or reflection high-energy electron diffraction. Efforts to combine techniques that measure surface structural defects with these that determine electronic properties would ap-

pear to be quite useful in resolving questions of this nature.

ACKNOWLEDGMENTS

We thank D. E. Savage and H. M. Clearfield for useful discussions. This research was supported by the U.S. Office of Naval Research.

- ¹F. Bartels, L. Surkamp, H. J. Clemens, and W. Mönch, *J. Vac. Sci. Technol. B* **1**, 756 (1983).
- ²W. Gudat and D. E. Eastman, *J. Vac. Sci. Technol.* **13**, 831 (1976).
- ³R. Ludeke, *Solid State Commun.* **21**, 815 (1977).
- ⁴H. Lüth, M. Büchel, R. Dorn, M. Liehr, and R. Matz, *Phys. Rev. B* **15**, 865 (1977).
- ⁵C. R. Brundle and D. Seybold, *J. Vac. Sci. Technol.* **16**, 1186 (1979).
- ⁶C. Y. Su, I. Lindau, P. R. Skeath, P. W. Chye, and W. E. Spicer, *J. Vac. Sci. Technol.* **17**, 936 (1980).
- ⁷P. W. Chye, C. Y. Su, I. Lindau, Perry Skeath, and W. E. Spicer, *J. Vac. Sci. Technol.* **16**, 1191 (1979).
- ⁸J. Stöhr, R. S. Bauer, J. C. McMenamin, L. I. Johansson, and S. Brennan, *J. Vac. Sci. Technol.* **16**, 1195 (1979).
- ⁹A. Kahn, D. Kanani, P. Mark, P. W. Chye, C. Y. Su, I. Lindau, and W. E. Spicer, *Surf. Sci.* **87**, 325 (1979); A. Kahn, D. Kanani, and P. Mark, *ibid.* **94**, 547 (1980).
- ¹⁰P. Mark, E. So, and M. Bonn, *J. Vac. Sci. Technol.* **14**, 865 (1977).
- ¹¹J. J. Barton, W. A. Goddard III, and T. C. McGill, *J. Vac. Sci. Technol.* **16**, 1178 (1979).
- ¹²P. Pianetta, I. Lindau, C. M. Garner, and W. E. Spicer, *Phys. Rev. B* **18**, 2792 (1978).
- ¹³P. Mark and W. F. Creighton, *Thin Solid Films* **56**, 19 (1979).
- ¹⁴G. Lucovsky, *J. Vac. Sci. Technol.* **19**, 456 (1981).
- ¹⁵J. J. Barton, C. A. Swarts, W. A. Goddard III, and T. C. McGill, *J. Vac. Sci. Technol.* **17**, 164 (1980).
- ¹⁶W. A. Goddard III, J. J. Barton, A. Redondo, and T. C. McGill, *J. Vac. Sci. Technol.* **15**, 1274 (1978).
- ¹⁷W. Mönch and R. Enninghorst, *J. Vac. Sci. Technol.* **17**, 942 (1980).
- ¹⁸E. J. Mele and J. D. Joannopoulos, *Phys. Rev. B* **18**, 6999 (1978).
- ¹⁹R. Ludeke, *Phys. Rev. B* **16**, 5598 (1977).
- ²⁰V. Heine, *Phys. Rev.* **151**, 561 (1966).
- ²¹P. J. Feibelman, E. J. McGuire, and K. C. Pandey, *Phys. Rev. B* **16**, 5499 (1977).
- ²²G. D. Davis and M. G. Lagally, *J. Vac. Sci. Technol.* **15**, 1311 (1978).
- ²³J. Tejeda, M. Cardona, N. J. Shevchik, D. W. Langer, and E. Schönherr, *Phys. Status Solidi B* **58**, 189 (1973); J. Tejeda, N. J. Shevchik, D. W. Langer, and M. Cardona, *Phys. Rev. Lett.* **30**, 370 (1973); J. C. Fuggle, L. M. Watson, P. R. Norris, and D. J. Fabian, *J. Phys. F* **5**, 590 (1975).
- ²⁴Purchased from Crystal Specialities, $\rho = 10^{-3} \Omega \text{ cm}$.
- ²⁵H. M. Clearfield and M. G. Lagally, *J. Vac. Soc. Technol. A* **2**, 844 (1984).
- ²⁶W. M. Mularie and W. T. Peria, *Surf. Sci.* **26**, 125 (1971).
- ²⁷J. E. Houston, *J. Vac. Sci. Technol.* **12**, 255 (1975).
- ²⁸H. H. Madden and J. E. Houston, *J. Appl. Phys.* **47**, 3071 (1976).
- ²⁹P. H. Van Cittert, *Z. Phys.* **69**, 304 (1931).
- ³⁰G. D. Davis, P. E. Viljoen, and M. G. Lagally, *J. Electron Spectrosc. Relat. Phenom.* **20**, 305 (1980).
- ³¹G. D. Davis, P. E. Viljoen, and M. G. Lagally, *J. Electron Spectrosc. Relat. Phenom.* **21**, 135 (1980).
- ³²The relative sensitivity factors for Ga and As were obtained from clean, cleaved GaAs, and that for O is from L. E. Davis, N. C. MacDonald, P. W. Palmberg, G. E. Riach, and R. E. Weber, *Handbook of Auger Electron Spectroscopy* (Physical Electronics Industries, Eden Prairie, Minnesota, 1976).
- ³³H. Gant and W. Mönch, *Surf. Sci.* **105**, 217 (1981).
- ³⁴K. D. Childs and M. G. Lagally, *J. Vac. Sci. Technol. A* **2**, 593 (1984).
- ³⁵K. D. Childs and M. G. Lagally (unpublished).
- ³⁶For oxygen coverages $\Theta > 0.8$, ML on the cleaved surface, we observe a slight increase [Ga]/[As] using the *MMM* lines that appears to be due to a changing secondary electron distribution caused by the O adsorption. This secondary electron distribution distorts the low-energy end of the Auger spectrum and thus also affects slightly the *MMM* lines, especially the As line, which occurs at ~ 30 eV.
- ³⁷The line shapes for cleaved GaAs in Ref. 22 are somewhat different from those presented here. We attribute these differences to slight contamination and to lower-quality cleaves for the measurements in Ref. 22. We find that adsorption of ambient species to a level of a few percent of a monolayer can change the line shapes in a direction to correspond more nearly to those of Ref. 22. The base pressure of the vacuum chamber is better by an order of magnitude for the present experiments and considerable care has been taken to improve the cleavage procedure. The data of Ref. 22 were taken with an intrinsic (semi-insulating) GaAs crystal, while the present data are taken with an *n*-type Te-doped crystal. Different dopants are known to affect the cleavage quality [W. Mönch and H. J. Clemens, *J. Vac. Sci. Technol.* **16**, 1238 (1979)].
- ³⁸M. Hansen and K. Anderko, *Constitution of Binary Alloys*, (McGraw-Hill, New York, 1958).
- ³⁹G. D. Davis, D. E. Savage, and M. G. Lagally, *J. Electron Spectrosc. Relat. Phenom.* **23**, 25 (1981).
- ⁴⁰O. Kubashewski and C. B. Alcock, *Metallurgical Thermochimistry* (Pergamon, Oxford, 1973).
- ⁴¹However, Ludeke's model (Ref. 3), if it were considered applicable up to saturation coverage, suggests a final oxygen coverage of $\Theta = 1.5$ ML. Our data show a marked decrease in the rate of adsorption for $\Theta \gtrsim 1$ ML.
- ⁴²D. E. Savage, D. Saloner, and M. G. Lagally (unpublished).
- ⁴³A. Guinier, *X-Ray Diffraction* (Freeman, San Francisco, 1963).
- ⁴⁴J. M. Blakely, *Introduction to the Properties of Crystal Surfaces* (Pergamon, Oxford, 1973).